

Supporting information for

## Trace Surface-Clean Palladium Nanosheets as a Conductivity Enhancer in Hole-Transporting Layers to Improve Overall Performances of Perovskite Solar Cells

Jing Cao,<sup>a</sup> Shiguang Mo,<sup>a</sup> Xiaojing Jing,<sup>a</sup> Jun Yin,<sup>a,b</sup> Jing Li,<sup>b</sup> and Nanfeng Zheng<sup>\*a</sup>

<sup>a</sup> State Key Laboratory for Physical Chemistry of Solid Surfaces, Collaborative Innovation Center of Chemistry for Energy Materials, and Engineering Research Center for Nano-Preparation Technology of Fujian Province, College of Chemistry and Chemical Engineering, Xiamen University, Xiamen 361005, China.

E-mail: nfzheng@xmu.edu.cn; Fax: +86-592-2183047.

<sup>b</sup> Pen-Tung Sah Institute of Micro-Nano Science and Technology, Xiamen University, Xiamen 361005, China.

### Experimental Section

#### Materials synthesis

The synthesis of Pd Nanosheets: In brief, 17 mg  $\text{Na}_2\text{PdCl}_4$  dissolved in 10 mL DMF, treated with 1 bar CO for 15 min under stirring. After 15 min, 1 mL  $\text{H}_2\text{O}$  was added without CO to obtain Pd Nanosheets seeds. After that, 70 mg  $\text{Pd}(\text{acac})_2$  was added to the Pd Nanosheets seeds and treated with CO to 1 bar, the temperature raised from room temperature to 60 °C in 60 min, and then kept for 90 min.

The synthesis of  $\text{CH}_3\text{NH}_3\text{I}$ : To a stirred solution of methylamine in methanol (40 wt%, 24 mL) was slowly added aqueous hydroiodic acid (57 wt%, 25 mL) at 0 °C. After 2 h, the precipitate was collected by evaporation at 50 °C for 1 h. The as-obtained product was washed with diethyl ether three times and then finally dried at 60 °C in a vacuum oven for 24 h to afford the desired pure  $\text{CH}_3\text{NH}_3\text{I}$  as white crystals.

#### Solar Cell Fabrication

Fluorine-doped Tin Oxide (FTO) glass substrates in the dimension of 2.0 cm × 2.0 cm were patterned by etching with zinc powder and 2 M hydrochloric acid. The substrates were then sequentially washed in ultrasonic baths of acetone, distilled water and ethanol. A compact  $\text{TiO}_2$  blocking layer was spin-coated onto the cleaned FTO glass using 0.15 M Titanium tetraisopropanolate in ethanol solution at 2000 rpm for 30 s. The substrate was heated at 120 °C for 15 min, and then annealed at 550 °C for 30 min. After cooling to the room temperature, the film was immersed into the 20 mM  $\text{TiCl}_4$  solution at 70 °C for 30 min. After dried, a ~200 nm thick mesoporous  $\text{TiO}_2$  film was deposited on the pre-treated FTO substrate by spin-coating of the  $\text{TiO}_2$  paste (Dyesol DSL 18NR-T) with ethanol (1:3, mass ratio), which was followed by the heating at 550 °C for 30 min. For the perovskite layer, a mixture of 461 mg of  $\text{PbI}_2$ , 159 mg of  $\text{CH}_3\text{NH}_3\text{I}$ , 78 mg of DMSO (molar ratio 1:1:1), and 600 mg of DMF was prepared at room temperature and stirred for 1 h. The completely dissolved precursor solution was spin-coated on the prepared substrate at

4000 rpm for 25 s, when 0.5 mL of diethyl ether was slowly dripped on the rotating substrate in 10 s. The obtained transparent film was then heated at 65 °C for 1 min and 100 °C for 2 min to form a dense CH<sub>3</sub>NH<sub>3</sub>PbI<sub>3</sub> film. P3HT or Spiro-OMeTAD solutions were then deposited on the perovskite layer by spin-coating their corresponding solutions at 4000 rpm for 30 s. In the deposition of HMLs, Spiro-OMeTAD solution was employed with 72.3 mg Spiro-OMeTAD, 28.8 μL of 4-tert-butyl pyridine and 17.5 μL of lithium bis(trifluoromethanesulfonyl)imide (Li-TFSI) solution (520 mg Li-TSFI in 1 mL acetonitrile) in 1 mL of chlorobenzene. P3HT solution was employed with 15 mg P3HT in 1 mL of chlorobenzene. For the fabrication of Pd-doped PSCs, Pd nanosheets were added in P3HT (from 0 to 0.15 wt%) and Spiro-OMeTAD (from 0 to 0.1 wt%) solutions. Finally, an 80 nm thick Au counter electrode was used by thermal evaporation under reduced pressure of  $2 \times 10^{-7}$  Torr. The active area was 0.10 cm<sup>2</sup>.

### Device Characterization

Current-voltage characteristics were recorded from a solar simulator equipped with a Keithley 2400 source meter and 300 W collimated Xenon lamp (Newport) calibrated with the light intensity to 100 mW·cm<sup>-2</sup> at AM 1.5 G solar light condition by the certified silicon solar cell. Incident photon-to-electron conversion efficiency (IPCE) was measured on a computer-controlled IPCE system (Newport) containing a Xenon lamp, a monochromator and a Keithley multimeter. The system was calibrated with the certified silicon solar cell and the IPCE data were collected at DC mode. XRD patterns were analyzed by an X-ray diffractometer (Rigaku, RINT-2500) with a CuKα radiation source. The surface morphology of were recorded via a SEM-4800 field-emission scanning electron microscope (SEM). The UV-vis spectra were measured with the perovskite infiltrated mesoscopic TiO<sub>2</sub> films supported by FTO glass using a Cary-5000 UV-Vis spectrophotometer. The photoluminescence spectra were measured using an Edinburgh Instruments FLS920 spectrometer. The electrochemical impedance spectroscopy (EIS) was carried out in the frequency range from 106 to 0.1 Hz in dark condition, in which the potential bias was applied at 800 mV. According to the simplified transmission line model, the arcs at high-intermediate frequency can be supposed to be charge-transport resistance. The conductivities of HTMs were measured in terms of space-charge-limited currents measurements by constructing optimized devices. The devices with a structure of ITO/PEDOT:PSS/HTM/Au were fabricated, and their *J-V* curves in the dark were obtained. The square resistances were carried out by Four-point probe measurement.

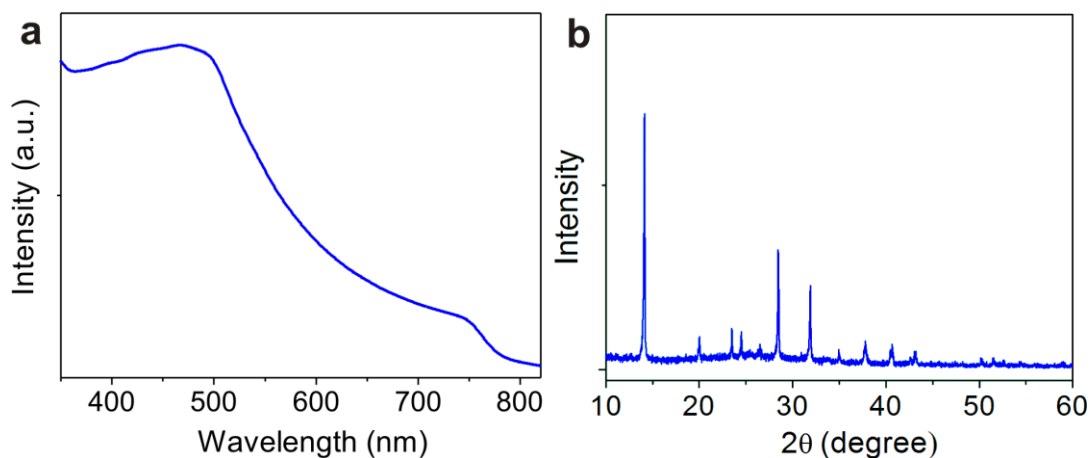


**Fig. S1.** The UV-vis (a) and XRD (b) spectra of perovskite film.

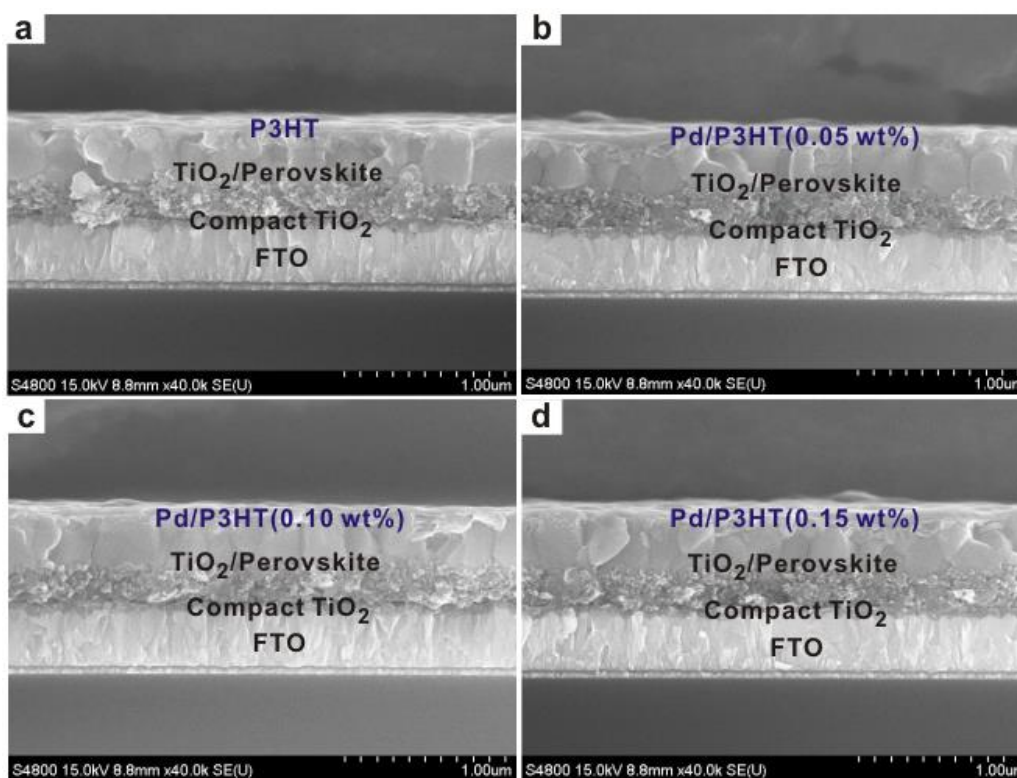


**Fig. S2.** SEM images of the films in different PSCs with (a) P3HT, (b) Pd/P3HT (0.05 wt%), (c) Pd/P3HT (0.10 wt%) and (d) Pd/P3HT (0.15 wt%).

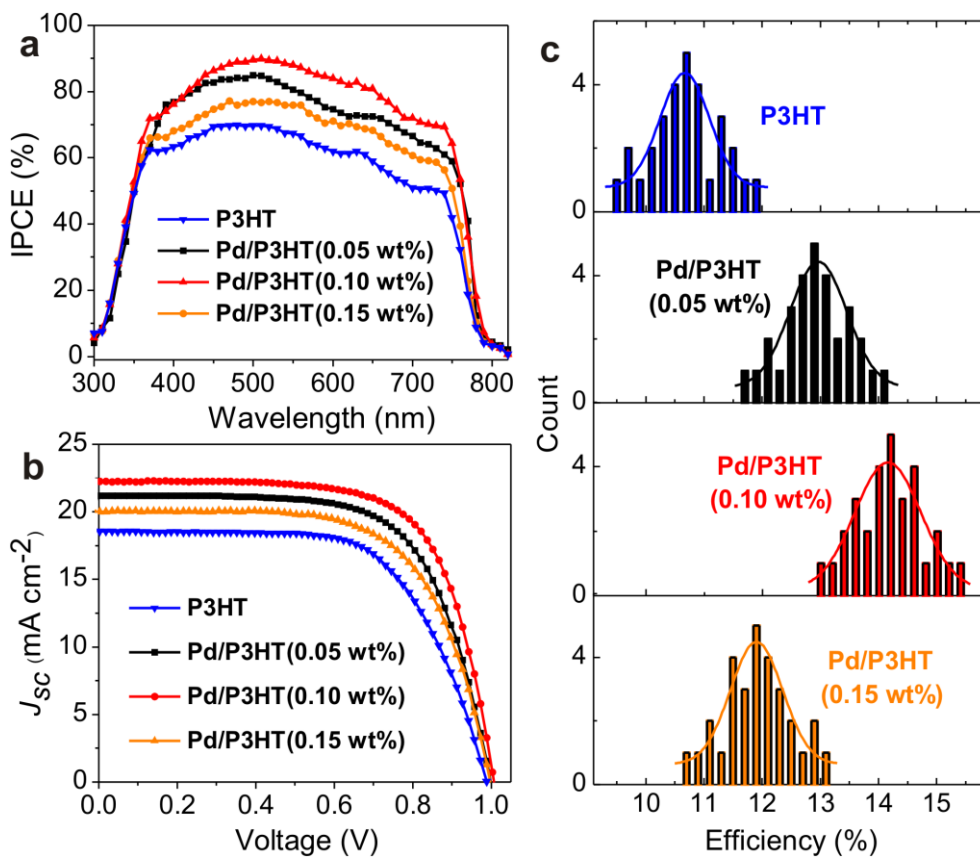


**Fig. S3.** The best IPCE (a), J-V (b) characteristics and comparison of the performance distributions of 30 individual devices (c) of the cells.

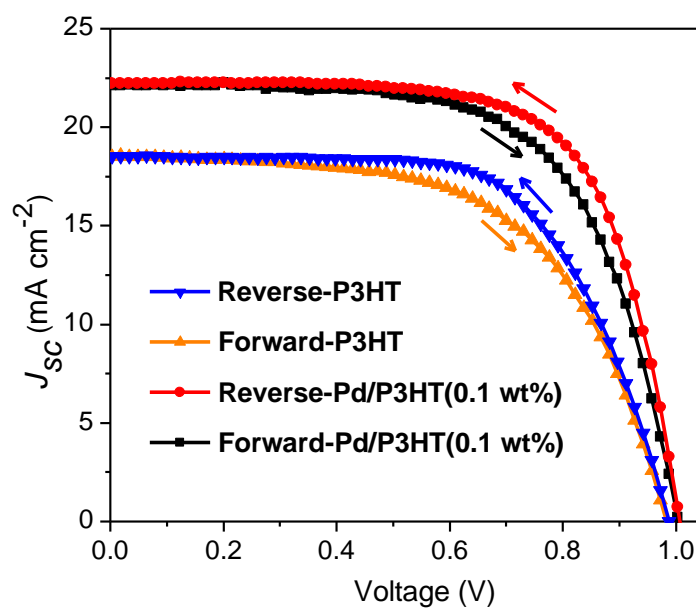


**Fig. S4.** The best J-V characteristics with both forward and reverse scans for the cells of P3HT and P3HT doped with Pd nanosheets (0.1 wt%).

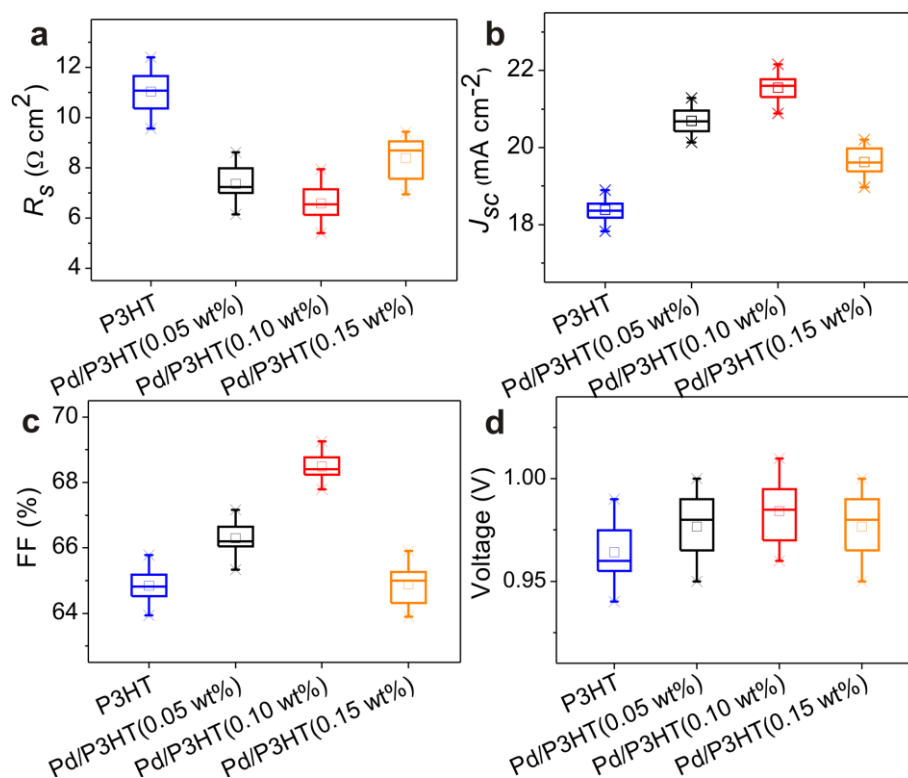


**Fig. S5.** Statistical data of 12 devices with P3HT and Pd/P3HT doped with Pd nanosheets on: (a-d) series resistance, short circuit current density, fill factor and open circuit voltage.

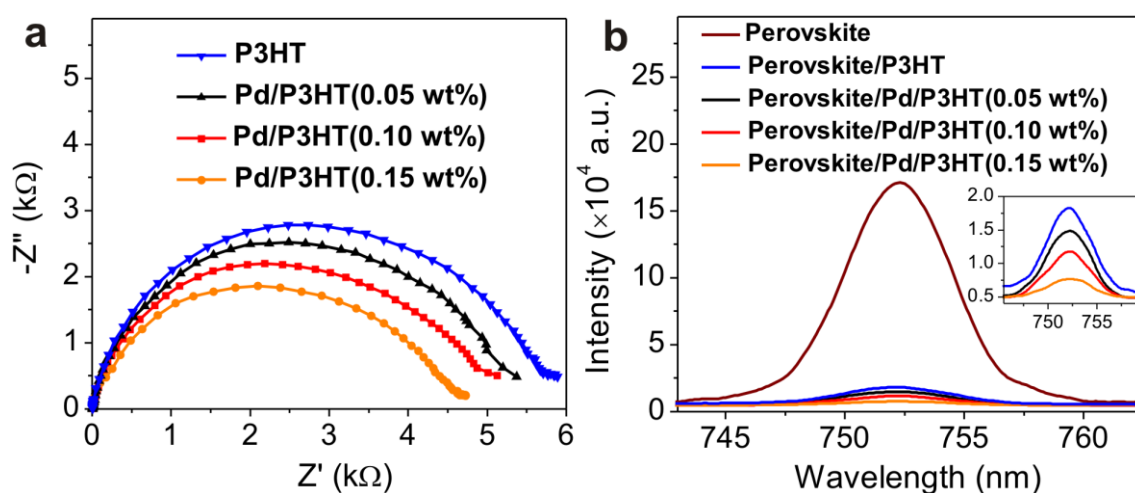


**Fig. S6.** (a) Nyquist plots of the devices in the dark at the 0.8 mV forward bias voltage. (b) Steady-state PL spectra of the films.

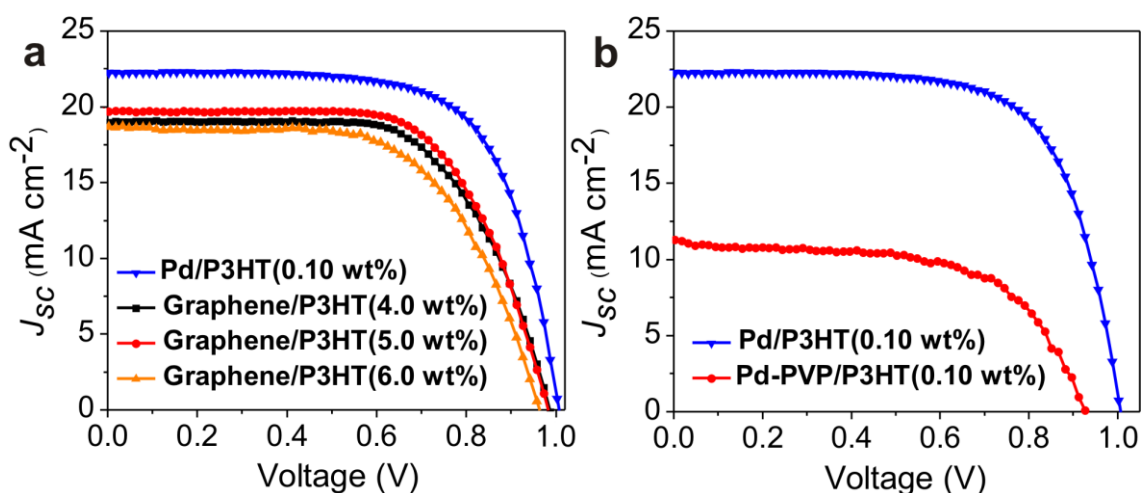


**Fig. S7.** The best J-V characteristics of (a) P3HT doped with graphene (graphene/P3HT) and Pd nanosheets (Pd/P3HT), and (b) P3HT doped with Pd nanosheets and Pd nanosheets protected by PVP (Pd-PVP/P3HT).

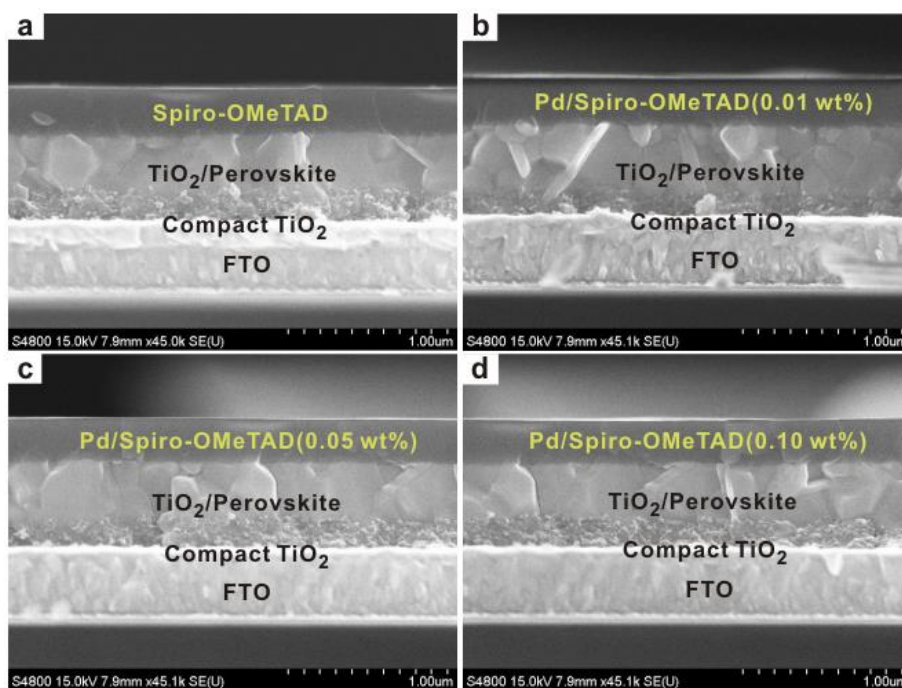


**Fig. S8.** The SEM images of the films with (a) Spiro-OMeTAD, (b) Pd/Spiro-OMeTAD (0.01 wt%), (c) Pd/Spiro-OMeTAD (0.05 wt%) and (b) Pd/Spiro-OMeTAD (0.10 wt%).

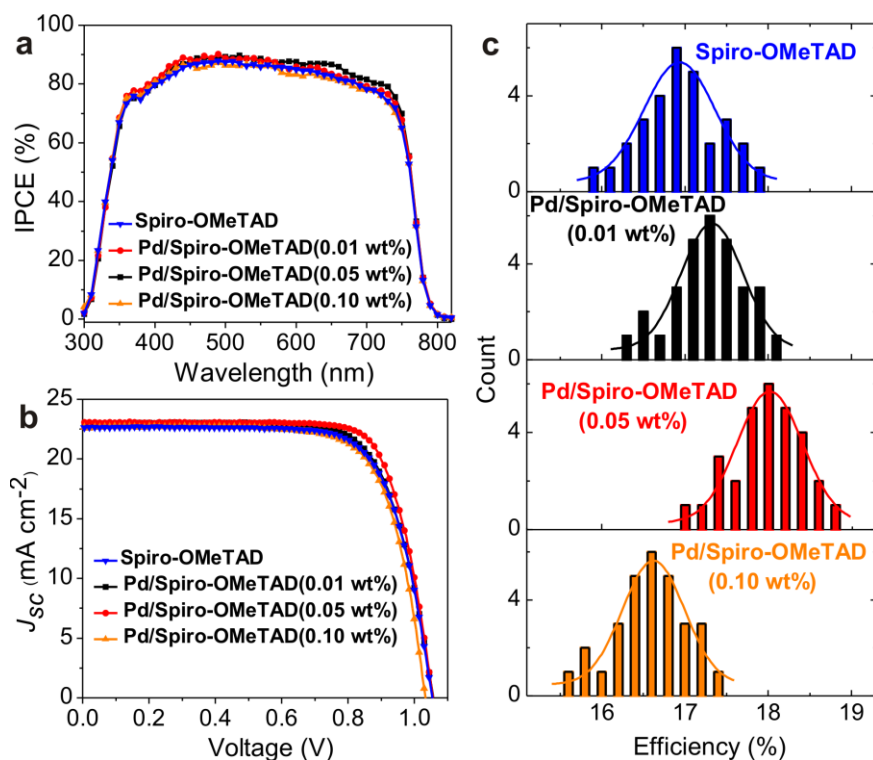


**Fig. S9.** The best IPCE (a),  $J$ - $V$  (b) characteristics and comparison of the performance distributions of 30 individual devices (c) of the cells.

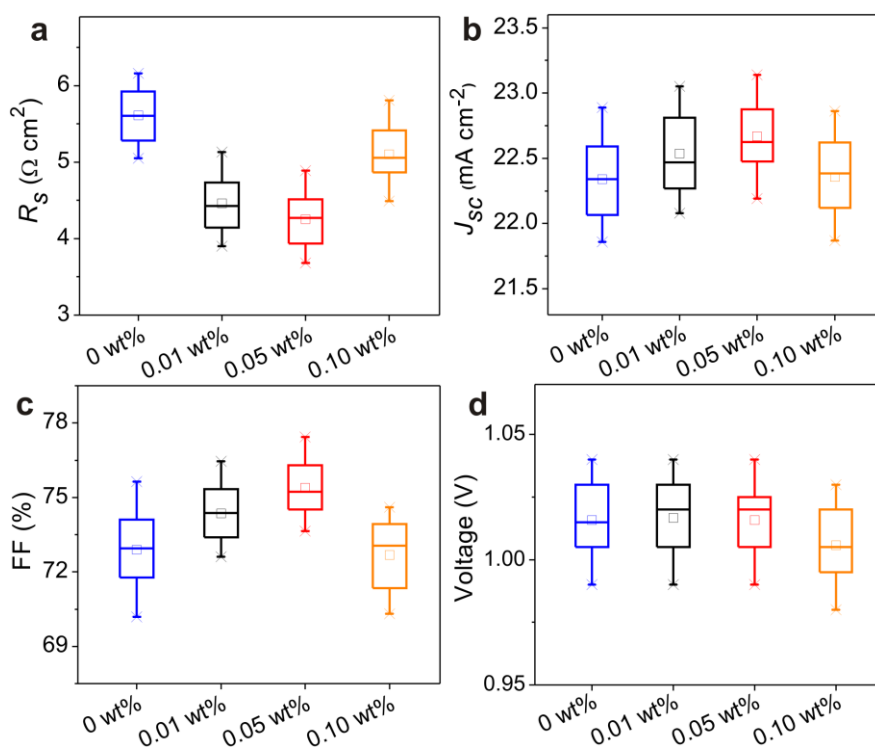


**Fig. S10.** Statistical data of 12 devices with Spiro-OMeTAD doped with different quality Pd nanosheets on: (a-d) series resistance, short circuit current density, fill factor and open circuit voltage.

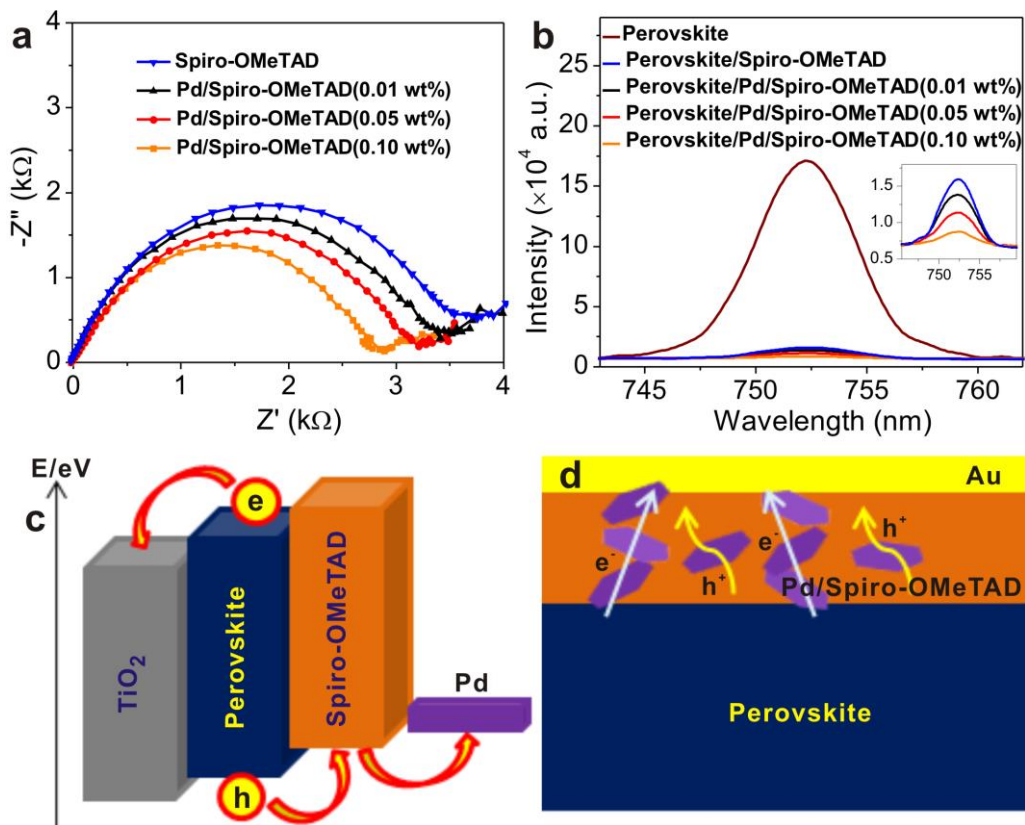


**Fig. S11.** (a) Nyquist plots of the devices in the dark at the 0.8 mV forward bias voltage. (b) Steady-state PL spectra of the films. (c) The energy level diagram of the materials used in PSCs. (d) Schematic of the interface of perovskite and HTM layers.

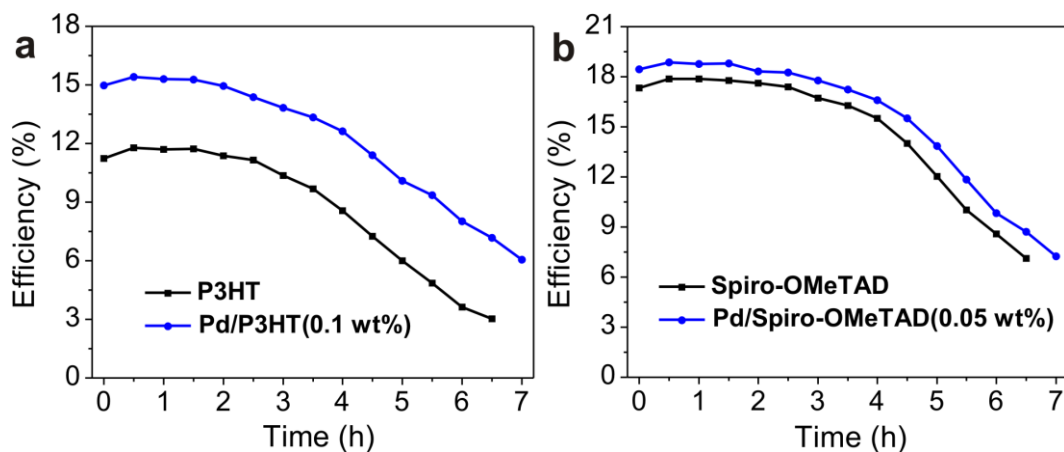


**Fig. S12.** The efficiency variation of the devices under illumination at AM 1.5 G with the humidity of 45%.

**Table S1.** Photovoltaic parameters of the cells with P3HT and P3HT doped with Pd nanosheets.

HTM	$J_{sc}/\text{mA}\cdot\text{cm}^{-2}$	$V_{oc}/\text{V}$	$FF/\%$	$\eta/\%$	$R_s/\Omega\cdot\text{cm}^{-2}$	Conductivity/ $\text{S}\cdot\text{cm}^{-1}$
P3HT	18.47	0.98	64.78	11.78	9.55	$3.1\times 10^{-4}$
Pd/P3HT(0.05 wt%)	21.18	1.00	66.84	14.12	6.36	$6.8\times 10^{-4}$
Pd/P3HT(0.10 wt%)	22.16	1.01	69.09	15.40	5.51	$9.4\times 10^{-4}$
Pd/P3HT(0.15 wt%)	20.04	1.00	65.44	13.06	7.11	$1.5\times 10^{-3}$

**Table S2.** Photovoltaic parameters derived from both forward and reverse scans for the cells with P3HT and P3HT doped with Pd nanosheets (0.1 wt%).

HTM		$J_{sc}/\text{mA}\cdot\text{cm}^{-2}$	$V_{oc}/\text{V}$	$FF/\%$	$\eta/\%$	$R_s/\Omega\cdot\text{cm}^{-2}$
P3HT	Reverse scan	18.47	0.98	64.78	11.78	9.55
	Forward scan	18.42	0.98	61.34	11.09	9.86
Pd/P3HT(0.1 wt%)	Reverse scan	22.16	1.01	69.09	15.40	5.51
	Forward scan	22.09	1.01	65.74	14.66	6.16

**Table S3.** Photovoltaic parameters of the cells with P3HT doped with graphene or Pd nanosheets protected by PVP.

HTM	$J_{sc}/\text{mA}\cdot\text{cm}^{-2}$	$V_{oc}/\text{V}$	$FF/\%$	$\eta/\%$	$R_s/\Omega\cdot\text{cm}^{-2}$
Pd/P3HT(0.10 wt%)	22.16	1.01	69.09	15.40	5.51
Graphene/P3HT(4.0 wt%)	19.04	0.98	67.07	12.57	8.86
Graphene/P3HT(5.0 wt%)	19.81	0.98	67.11	13.06	8.65
Graphene/P3HT(6.0 wt%)	18.73	0.96	61.79	11.15	9.44
Pd-PVP/P3HT(0.10 wt%)	11.26	0.93	59.53	6.21	12.98

**Table S4.** Photovoltaic parameters of the cells with Spiro-OMeTAD and Spiro- OMeTAD doped with Pd nanosheets.

HTM	$J_{sc}/\text{mA}\cdot\text{cm}^{-2}$	$V_{oc}/\text{V}$	$FF/\%$	$\eta/\%$	$R_s$ $/\Omega\cdot\text{cm}^{-2}$	Conductivity $/\text{S}\cdot\text{cm}^{-1}$
Spiro-OMeTAD	22.84	1.05	74.24	17.88	5.12	$4.5\times 10^{-3}$
Pd/Spiro-OMeTAD (0.01 wt%)	23.01	1.05	74.57	18.06	4.54	$5.9\times 10^{-3}$
Pd/Spiro-OMeTAD (0.05 wt%)	23.18	1.05	77.09	18.86	4.43	$7.1\times 10^{-3}$
Pd/Spiro-OMeTAD (0.10 wt%)	22.78	1.03	73.81	17.36	4.89	$8.9\times 10^{-3}$